ONECENTRAL PRESS

Available online at www.onecentralpress.com

One Central Press

journal homepage: www.onecentralpress.com/nano-energy-systems

Modification and application of 1D nanostructure in DSSC and PSC

*Yang Xu, Jinshu Wan, Baoyuan Wang, Jinxia Duan, Jun Zhang, Hao Wang**

Hubei Collaborative Innovation Center for Advanced Organic Chemical Materials,
Hubei Key laboratory of ferroelectric and dielectric materials and devices,
Faculty of Physics and Electronic Science, Hubei University, Wuhan 430062, China.
**Corresponding author*

ABSTRACT

1-dimensional (1D) nanostructured photoanode and electron transport material (ETL) such as nanotubes and nanorods, have developed as excellent choices for Dye-sensitized solar cell (DSSC) and perovskite solar cell (PSC) due to their advantages of direct electron-transport path, excellent electron collect and transport ability. What's more, extra superficial area, better interface contact and energy-level decoration can also be realized through surface modification. Here, we review our progress on the DSSC and PSC based on 1D nanostructure including basic structure, working principle, surface morphology before and after specific treatment together with corresponding performance and fundamental mechanism.

Highlights

1. $TiCl_4$ treatment is efficient for solar cells based on 1D TiO_2 nanostructure
2. Co-sensitization method can be a route to acquire higher efficiency
3. ETL/perovskite interface contact is vital for Cell performance.

I. INTRODUCTION

DSSC and PSC have attracted many interests for their potential of acquiring low cost renewable solar energy. Although the light absorbers are different, these two types of cells share many similar characteristics. As can be seen in Fig. 1 (a) and (c), classic DSSC is composed by dye molecule covered N type nanocrystalline with high specific surface area ratio as photoanode, redox electrolyte and counter electrode [1]. At the same time, typical PSC is combined with N type semiconductor compact layer and scaffold layer that act as ETL when functioning. Then a layer of perovskite crystal is infiltrated into the scaffold layer as absorber, it should also be noticed that the thickness of the perovskite layer greatly depends on the scaffold layer thickness. Finally, hole transport layer (HTL) and a layer of counter electrode is attached onto the top [2]. Fig. 1(b) and (d) shows the basic principle for these two types of solar cells. When the absorbers receive sun light, a large number of electrons and holes are generated. The electron path is similar, they will be collected by the photoanode or ETL and transport to the substrate. After the external circuit, electrons will experience a series of redox reactions before returning to the dye [1]. While for PSC, perovskite generated holes will pass to the HTM through valance band and then to the counter electrode [3].

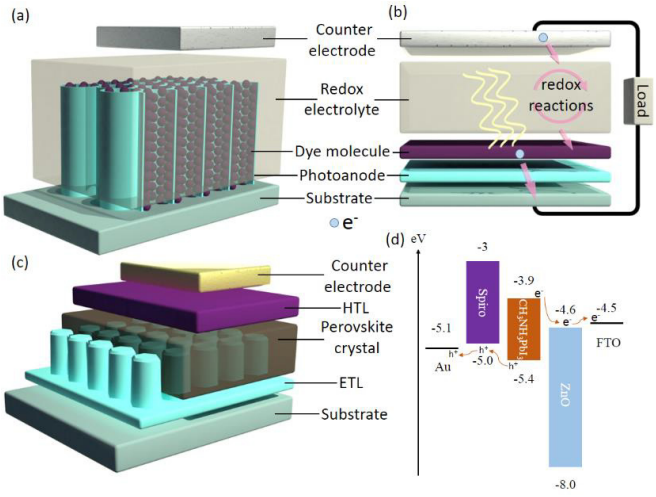

Figure 1 (a) Schematic configuration of DSSC, (b) basic working principle of DSSC, (c) Schematic configuration of PSC, (d) basic working principle of PSC.

II. 1D NANOSTRUCTURE IN DSSC AND PSC

In our works, we mainly concentrate on the 1D nanostructured photoanode and ETL such as nanotubes and nanorods. Fig. 2 are the combine of cross section SEM image for nanotubes and nanorods. For DSSC with 1-dimensional TiO_2 nanotubes, the precise control of electrochemical anodic oxidation process result in tightly arranged length tunable nanotubes with similar sized holes, which can be seen from Fig. 2(a). To meet the demand for high specific surface area, DSSC with different length of TiO_2 nanotubes have been tested and a 33 μm long TiO_2 nanotubes shows the highest efficiency of 4.86 % [1] which is given in table 1.1. As mentioned above, the increase of the superficial area has a positive relationship with dye loading and further raise the efficiency performance mainly through short-circuit current density (J_{sc}) improvement. Fig. 2(b) shows the surface SEM image of TiO_2 nanotubes after $TiCl_4$ treatment, TiO_2 nanoparticles of diameter close to 20 nm have been successfully introduced for the superficial area expansion since the hydrolysis products of the $TiCl_4$ are TiO_2 and HCl. The TEM image of untreated and treated TiO_2 nanotubes in Fig. 3 suggest that the inner part of TiO_2 nanotubes are fully covered with TiO_2 nanoparticles. Additional quantization of the treatment effect is held by Brunauer-Emmett-Teller (BET) and Desorption test. Both the dye adsorption and evaluated inner surface area are ~ 2.23 times larger than pure nanotubes. Obviously, this calculation ensures that the dye is complete attached onto the whole inner surface of the nanotubes and confirms the treating effect again. As a result, J_{sc} has an increase of about 1 time than the untreated samples and cell efficiency gains up to 9.86 % [4].

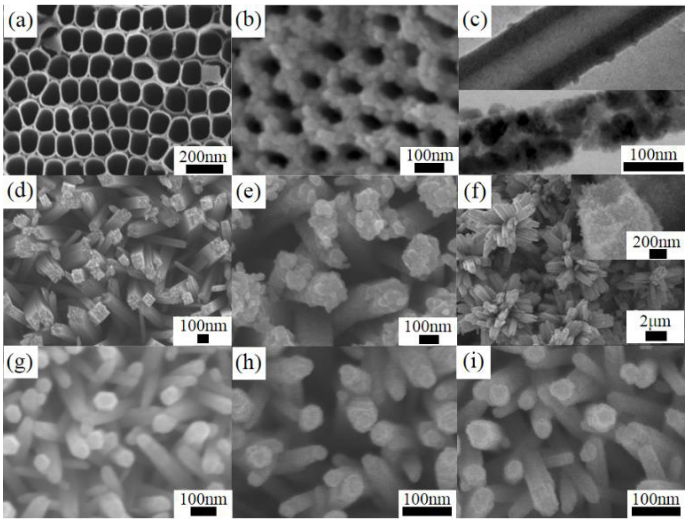

Figure 2 SEM image of (a) pure TiO_2 nanotubes with average length of 33 μm [1]; (b) TiO_2 nanotubes after $TiCl_4$ treatment [4]; (d) bare TiO_2 nanorods with average length of 4 μm [5]; (e) CdS covered TiO_2 nanorods [5]; (f) $TiCl_4$ modified 1D nanorods/3D nanotubes [6]; (g) bare ZnO nanorods with average length of 600 nm [7]; (h) bare ZnO nanorods with average length of 400 nm [7]; (i) PCBM modified ZnO nanorods with average length of 1 μm [2]. TEM image of upper (c) pure TiO_2 nanotube and lower (c) TiO_2 nanotube after $TiCl_4$ treatment [4].

For DSSC based on hydrothermal method made TiO_2 nanorods, Fig. 2(d) shows pure anatase phase TiO_2 nanorods (average length of ~ 4μm) that shaped as square column with smooth side surface and covered by small protuberances. Fig. 2(e) describe the surface appearance of TiO_2 nanorods coated with CdS shell structure that plays as the role of light absorber. The quantum dot sensitized samples receive 1.08 % through a solar simulator. For further improvement on the cell performance, CdS/dye co-sensitized solar cell is fabricated and efficiency reaches to 2.81 % [5]. What should be mentioned is that the two kinds of sensitizer can cooperate efficiently, suggesting that such co-sensitization methods can be a route for performance acceleration. Another trial has been conducted by adding a layer of 3D flower like TiO_2 nanorods onto the top of pure TiO_2 nanorods for more superficial area. As Fig. 2(f) shows, 3D TiO_2 nanotubes are the result of $TiCl_4$ etched 3D flower like TiO_2 nanorods. Inset of Fig. 2(f) is a detailed image of $TiCl_4$ treated 3D TiO_2 nanotubes with its inside and outside surface covered by a mass of TiO_2 nanoparticles. The dye loading of the combination of 1D nanorods/3D nanotubes are 3.58 times higher than the 1D/3D nanorods and 1.7 times of the 3D nanotubes through a desorption test. Further EIS test also indicates that the 1D nanorods/3D nanotubes exhibit lowest series resistance and electron transfer resistance, which can minimize their negative influence on the FF (fill factor) and J_{sc}. With the combine of the highest superficial area and lowest resistance data, final efficiency reaches to 7.68 % [6] as table 1.5 shows.

Owing to the ultrahigh absorption coefficient, perovskite crystal can effectively absorb the sun light with extremely thin layer. Fig. 2(g) is the cross-section SEM image of 600 nm long ZnO scaffold nanorods. Similar as normal nanorods, these lead zinc ore ZnO nanorods have hexagon shaped top with relatively smooth side surface. Further experiment indicates that the surface roughness of the nanorods have an inverse relationship with rod length. Shorter nanorods as Fig. 2(h) (average length of ~ 400 nm) shows rougher surface appearance which is far from normal ZnO nanorods. However, smooth surface nanorods are not suitable for perovskite attachment due to the serious charge recombine phenomenon. Even though the relatively longer nanorods do help increase the perovskite loading and J_{sc} at a certain extent, the decrease of the open-circuit voltage (V_{oc}) dominate the cell performance and lower the efficiency [7]. To make longer nanorods rougher, PCBM was spun onto the longer nanorods (average length of ~ 1 μm). The little dot that attached onto the surface of nanorods as Fig. 2(i) shows are the PCBM. Cell efficiency for PCBM decorated PSC is 11.67 % which we believe is in fact the combination of the rougher surface, increased absorber loading and the conduction band modification. Since the conduction band of PCBM locate just between the conduction band of perovskite and ZnO nanorods, which makes

the PCBM serve as the ladder for electrons during the injection process from perovskite to ZnO nanorods [2].

III. SUMMARY AND OUTLOOK

In conclusion, to achieve higher efficiency through enhancing the specific surface area ratio and absorber loading based on 1D metallic oxide structure is practicable. Chemical properties of materials should be taking into account when choosing specific treatment. $TiCl_4$ treatment are widely used due to its hydrolysis products that have the ability to enhance superficial area, attach additional TiO_2 nanoparticles and roughen the surface appearance through acid etching at the same time. However, the extremely low pH stability of ZnO makes it only fit for mild treatments instead of etching methods, which do limits its application somehow. On the other hand, V_{oc} for samples after surface treatment have some increase regardless of the materials used for absorber, photoanode or ETL, which suggesting the importance of interface contact and attachment. Clearly, treatments that means for extra superficial area are suitable for the sensitized solar cell and may sometimes increase both J_{sc} and V_{oc} since the absorber loading quantity and its attachment are critical.

Table 1 Summary of different types of cells.

Cell Structure	V_{oc} (V)	J_{sc} (mA/cm2)	FF	Eff (%)	Ref
1. FTO/TiO_2 nanotubes/Dye/Iodide electrolyte/Pt	0.63	11.47	66.8	4.86	[1]
2. FTO/$TiCl_4$ treated TiO_2 nanotubes/Dye/Iodide electrolyte/Pt	0.71	24.78	56.0	9.86	[4]
3. FTO/TiO_2 nanorods/CdS shell/Iodide electrolyte/Pt	0.69	4.9	32.0	1.08	[5]
4. FTO/TiO_2 nanorods/CdS shell/Dye/Iodide electrolyte/Pt	0.67	11.25	38.0	2.81	[5]
5. FTO/TiO_2 nanorods/3D TiO_2 nanotubes/Dye/Iodide electrolyte/Pt	0.72	18.3	58.3	7.68	[6]
6. FTO/ZnO nanorods (600 nm)/CH3NH3PbI3/Spiro-oMeTAD/Au	0.89	18.3	47.2	7.72	[7]
7. FTO/ZnO nanorods (410 nm)/CH3NH3PbI3/Spiro-oMeTAD/Au	0.96	17.8	54.0	9.15	[7]
8. FTO/ZnO nanorods (1 μm)/PCBM/CH3NH3PbI3/Spiro-oMeTAD/Au	0.96	22.1	55.2	11.67	[2]

IV. ACKNOWLEDGEMENTS

This work is supported in part by the National Nature Science Foundation of China (No. 51372075).

V. REFERENCES

[1] J. Zhang, S. Li, H. Ding, Q. Li, B. Wang, X. Wang, H. Wang, J. Power Sources 247 (2014) 807-812.
[2] Y. Xu, Y. Wang, J. Yu, B. Feng, H. Zhou, J. Zhang, J. Duan, X. Fan, P.A.V. Aken, P.D. Lund, H. Wang, IEEE J. Photovolt. 6 (2016) 1530-1536.
[3] S. Kazim, M.K. Nazeeruddin, M. Grätzel, S. Ahmad, Angew. Chem. Int. Edit. 53 (2014) 2812–2824.
[4] J. Zhang, Q. Li, S. Li, Y. Wang, C. Ye, P. Ruterana, H. Wang, J. Power Sources 268 (2014) 941-949.
[5] B. Wang, H. Ding, Y. Hu, H. Zhou, S. Wang, T. Wang, R. Liu, J. Zhang, X. Wang, H. Wang, Int. J. Hydrogen Energy 38 (2013) 16733-16739.
[6] H. Wang, B. Wang, J. Yu, Y. Hu, C. Xia, J. Zhang, R. Liu, Sci. Rep. 5 (2015).
[7] Y. Xu, T. Liu, Z. Li, B. Feng, S. Li, J. Duan, C. Ye, J. Zhang, H. Wang, Appl. Surf. Sci. 8 (2016) 89-96.